

New Measurements of Orbital Period Change in Cygnus X-3

N. S. Singh¹, S. Naik², B. Paul², P. C. Agrawal², A. R. Rao² and K. Y. Singh¹

¹ Dept. of Physics, Manipur University, Canchipur, Imphal 795003, Manipur, India

² Tata Institute of Fundamental Research, Homi Bhabha Road, Mumbai 400005, India

the date of receipt and acceptance should be inserted later

Abstract. A nonlinear nature of the binary ephemeris of Cygnus X-3 indicates either a change in the orbital period or an apsidal motion of the orbit. We have made extended observations of Cygnus X-3 with the Pointed Proportional Counters (PPCs) of the Indian X-ray Astronomy Experiment (IXAE) during 1999 July 3–13 and October 11–14. Using the data from these observations and the archival data from ROSAT, ASCA, BeppoSAX and RXTE, we have extended the data base for this source. Adding these new arrival time measurements to the published results, we make a comparison between the various possibilities, (a) orbital decay due to mass loss from the system, (b) mass transfer between the stars, and (c) apsidal motion of the orbit due to gravitational interaction between the two components. Orbital decay due to mass loss from the companion star seems to be the most probable scenario.

Key words. binaries: close – stars: individual: Cygnus X-3 – stars: Wolf-Rayet – X-rays: stars

1. Introduction

The nature of the compact object in the bright X-ray binary Cygnus X-3, is a subject of much debate. In spite of being one of the most frequently observed X-ray sources, presence of an X-ray pulsar, a black hole, or a low magnetic field neutron star has not yet been established. There is also uncertainty about the mass and type of the companion star. An interesting way to probe this system is to investigate the arrival time history of the 4.8 hr orbital modulation in the X-ray light curve.

The unusual X-ray binary Cygnus X-3 is located in the plane of our galaxy at a distance of > 11.6 kpc (Dickey 1983). Because of the high luminosity of the source in X-ray, infrared and radio bands, it has been observed on many occasions at these wavelengths. Strong optical extinction in the direction of the source prevents optical observations. The mass of the companion star has been determined by many different means and it is found to be in the range of a fraction of solar mass to a few solar mass (Van den Heuvel & De Loore 1973; Tavani, Ruderman, & Shaham 1989; van Kerkwijk et al. 1992). Parsignault et al. (1976) discovered a periodicity of 4.8 hr in the X-ray flux with nearly sinusoidal variation, which is believed to be due to the orbital motion. The variation in the sinusoidal shape of the light curve from cycle to cycle is reported by van der Klis and Bonnet-Bidaud (1981). They showed that the shape of the average light curve formed from successive cycles is quasi-sinusoidal with a slow rise and fast fall.

Several models have been proposed to explain the deep and near-sinusoidal modulation of the X-ray intensity of Cygnus X-3 with the orbital period (Ghosh et al. 1981). Material in the form of a large shell around the binary system can produce the X-ray modulation by scattering, absorbing, and re-emitting the X-rays from the compact object, if the X-ray emission is only from the non-shadowed part of the shell. White & Holt (1982) proposed the accretion disk corona (ADC) model to explain the modulation in the X-ray light curve of the source. According to this model, the X-ray source is covered by an optically thick corona with a radius of about 10^9 cm, an optical depth of about 10 and a temperature of about 2 keV. Another model which tries to explain the orbital modulation is stellar wind model (Willingale, King, & Pounds 1985; Kitamoto et al. 1987). This model assumes a strong and highly ionized stellar wind from the companion star with an optical depth of about 1 and a radius of about 10^{11} cm and the temperature of the wind is model dependent.

Evolution of the orbit of Cygnus X-3 is studied by measuring the arrival times of the minima in each orbital motion. The ephemeris of 4.8 hr modulation in the X-ray light curve of the source has been studied by many authors (Leach et al. 1975; Mason & Sanford 1979; Parsignault et al. 1976; Lamb, Dower & Fickle 1979; Elsner et al. 1980; van der Klis & Bonnet-Bidaud 1981, 1989; Kitamoto et al. 1987). The time derivative of the orbital modulation period (\dot{P}) and second derivative (\ddot{P}) have been measured as $\sim 10^{-9}$ s s⁻¹ and $\sim -10^{-11}$ yr (van der Klis & Bonnet-Bidaud 1981, 1989; Kitamoto et al. 1987). The unusually

large value of \dot{P}/P ($= 2.2 \times 10^{-6} \text{ yr}^{-1}$), which if linked to the binary evolution of the system, is similar to several short-period bright LMXBs such as X1822–371 with $\dot{P}/P \sim 3.4 \times 10^{-7} \text{ yr}^{-1}$ and orbital period of 5.57 hr (Hellier et al. 1990; Parmar et al. 2000), EX00748–767 with $\dot{P}/P \sim 2 \times 10^{-7} \text{ yr}^{-1}$ and orbital period of 3.82 hr (Parmar et al. 1991). This value of \dot{P} can be interpreted as due to the mass transfer from the optical companion to the compact object. Using the measured period derivative of Cygnus X–3, Kitamoto et al. (1987) determined the rate of mass loss from the binary companion as about $10^{-6} M_{\odot} \text{ yr}^{-1}$. Tavani et al. (1989) tried to explain the observed high value of \dot{P}/P in Cygnus X-3 and the required mass transfer rate close to $\sim 1.58 \times 10^{-8} M_{\odot} \text{ yr}^{-1}$. They claimed that the companion is a degenerate star with solar composition and in the mass range of $0.01 \leq m \leq 0.03 M_{\odot}$ which under-fills its Roche lobe. The X-ray illumination from the primary compact object produces the evaporative wind from such a low-mass degenerate companion. However, from infrared observations, van Kerkwijk et al. (1992) discovered that the binary companion of Cygnus X-3 has the spectrum of a Wolf-Rayet star and predicted the mass of the companion as $\sim 10 M_{\odot}$ which suggests that Cygnus X-3 is a high mass X-ray binary. Recent observations by Fender et al. (1999) confirm the nature of the companion as an early-type WN Wolf-Rayet star.

We have measured the available arrival time of minimum value of the light curve from two observation of Cygnus X-3 with PPCs of IXAE in 1999 and several archival data. By combing these new measurements with the previously published results, we are able to determine the rate of change of orbital period with greater accuracy.

2. Observations and Archival Data

2.1. PPC Observations

The X-ray observations of Cygnus X-3 were carried out twice on 1999 July 3–13 and 1999 October 11–14 with 1 s time-integration mode with the PPCs of the IXAE on board the Indian satellite IRS-P3. The IXAE includes three co-aligned and identical, multi-wire, multi-layer proportional counters with a total effective area of 1200 cm^2 covering 2 to 18 keV energy range with an average detection efficiency of about 60% in 3–7 keV energy range. Each PPC is equipped with a honeycomb type collimator having a field of view of $2^{\circ}.3 \times 2^{\circ}.3$ and has an overall energy resolution of about 22% at 6 keV (Agrawal et al. 1998; Rao et al. 1998). The IRS-P3 satellite is in a circular orbit at an altitude of 830 km and inclination of 98° . Pointing towards any particular source is done by using a star tracker with an accuracy of $\leq 0^{\circ}.1$. The useful observation time is limited to the latitude range typically from 30°S to 50°N to avoid the rise in charged particle background at high latitudes. The South Atlantic Anomaly (SAA) region restricts the observation to 5 of the 14 orbits per day. As the detectors are co-aligned, simultaneous background observation is not possible. The background

counts are measured after the observation of a source by pointing the PPCs to a source-free region in the sky, close to the target source. The total useful exposure time of the X-ray source during the two observations is 31245 s. The PPC light curves did not show strong intensity variations on the time scale of a few seconds to a few hundred seconds.

2.2. Archival data

We have also analyzed archival data from several satellites. From ROSAT mission, we have analyzed HRI data with two different observation IDs. The durations of these two observations are inter-wined, but the overall count rate is different because in one of the observations, the source was near the edge of the field of view where effective area is small. RXTE/PCA observations of the source in 2–60 keV energy range, combined data from GIS detectors (GIS2 and GIS3) and SIS detectors (SISO and SIS1) of the ASCA satellite and data from MECS detectors of BeppoSAX observations were used to determine more arrival time information of Cygnus X–3. We have analyzed the RXTE/ASM dwell data in the energy range of 2–12 keV for the entire period of observation starting from 1996 January to 2001 August 30. The details of the observations of the source with different satellites are given in Table 1 along with the useful exposure period.

Table 2. Archival data used for the determination of the arrival time of the minima of the binary modulation

Satellite	Date of observation	Exposure (in seconds)	Detector
ASCA	1994 29/5 – 30/5	21468	GIS
ASCA	1994 29/5 – 30/5	17527	SIS
ROSAT	1995 20/4 – 22/4	72709	HRI
ROSAT	1995 21/4 – 23/4	51670	HRI
BeppoSAX	1996 22/9 – 24/9	51626	MECS
BeppoSAX	1996 10/10	26167	MECS
BeppoSAX	1996 29/10	13664	MECS
BeppoSAX	1997 19/9 – 20/9	25802	MECS
RXTE	1996 24/8 – 30/8	86450	PCA
RXTE	1997 16/2 – 22/2	59465	PCA
RXTE	1997 05/6 – 26/9	64693	PCA
RXTE	1998 16/5 – 21/5	34723	PCA
RXTE	1996 04/1 –		
	2001 30/8		ASM

3. Data Analysis and Results

3.1. Arrival time determination

The data used for the analysis were corrected to the solar system barycenter. To avoid the cycle to cycle variation in the light curve, we have created the time averaged orbital

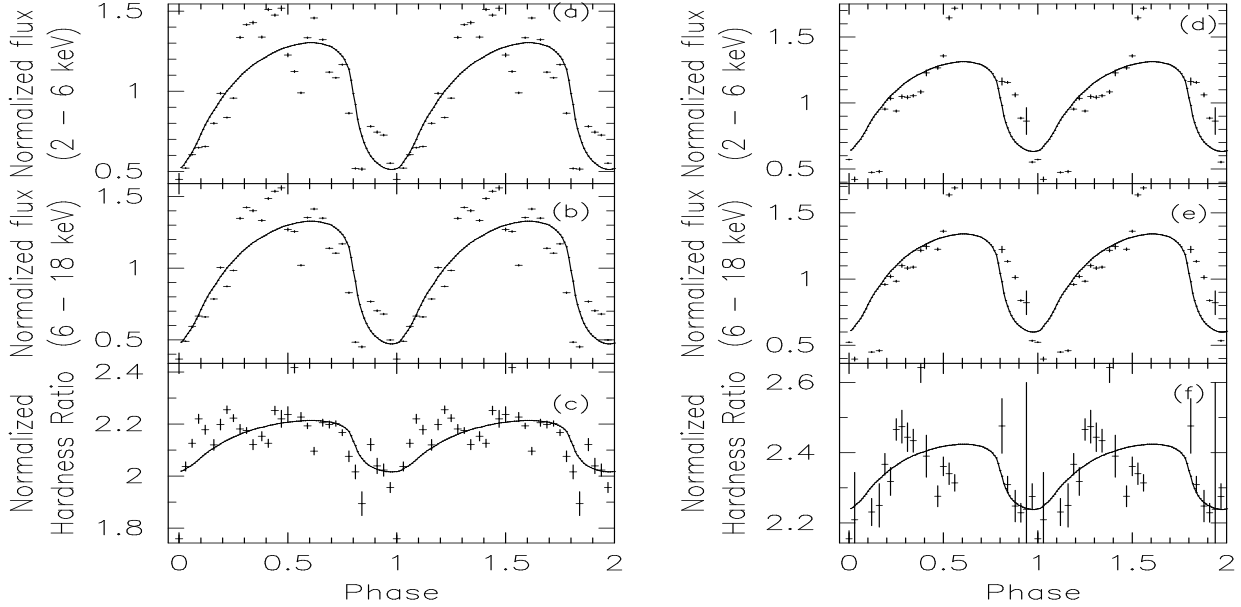


Fig. 1. Folded light curves in 2–18 keV and 6–18 keV energy ranges are shown in the panels (a) and (b) (for 1999, July 3–13 PPC observations) and panels (d) and (e) (for 1999, October 11–14 PPC observations) on a normalized scale with the template data (described in text) which is indicated by lines. The panels (c) and (f) show the folded hardness ratios (ratio of the count rate in 6–18 keV energy range to the count rate in 2–6 keV energy range for 1999, July and October observations respectively).

modulation profile by folding the source light curves with a period of 17253 seconds (Elsner et al. 1980). In all cases, the shape of the folded light curves is somewhat similar to the shape of the template function which is the long term average shape of the light curve obtained with the Copernicus satellite (Mason et al. 1976).

To determine the arrival times of the minimum of the folded light curves, we have used the normalized template data of X-ray ephemeris of Cygnus X-3 (van der Klis et al. 1989). The folded data were cross-correlated with the standard template function as described by van der Klis et al. (1989) to get the phase difference in the minima of the template and the data which give the measure of the arrival time of the minima. In addition to the statistical variations, Cygnus X-3 often shows some short-term intensity variations superposed on the orbital modulation. We have multiplied the statistical error estimates of each folded light curve by some constant factors to make them fit to the template with a reduced χ^2 of 1.0. The error in the arrival times were estimated from the uncertainties in determining the center of the Gaussian function of the cross-correlated data. The short-term occasional intensity variations also cause some random fluctuations in the arrival time determinations. Following the earlier works (Kitamoto et al. 1995), we have quadratically added 0.002

d to the arrival uncertainties to make them compatible with the previous reported measurements.

This analysis yielded two new arrival points from PPC observations (Singh et al. 2001), two points from ASCA, two points from ROSAT, five points from RXTE/PCA, and four points from BeppoSAX observations. We divided the RXTE/ASM light curve into 19 segments of durations of 100 days as given in Table 2, and determined the arrival times from each data segment. The information regarding the new arrival times are given in Table 1 along with the observation periods of the source with different instruments on different satellites and the orbit number. In accordance with the earlier works (Leach et al. 1975), we have assigned the orbit number of the source as 0 at JD 2440949.9201. The orbit numbers for later observations were calculated by using 4.8 hour orbital period of the source. The significant increase in the number of the new arrival points to the old data improved the numerical values of the period derivative and the double derivative.

The orbital modulation of the light curves obtained from the observations of the source with different instruments are shown in different figures along with the normalized template. Panel (a) and (d) of Figure 1 show the folded light curves in 2–18 keV energy range along with the normalized template for 1999 July 3–13 and 1999

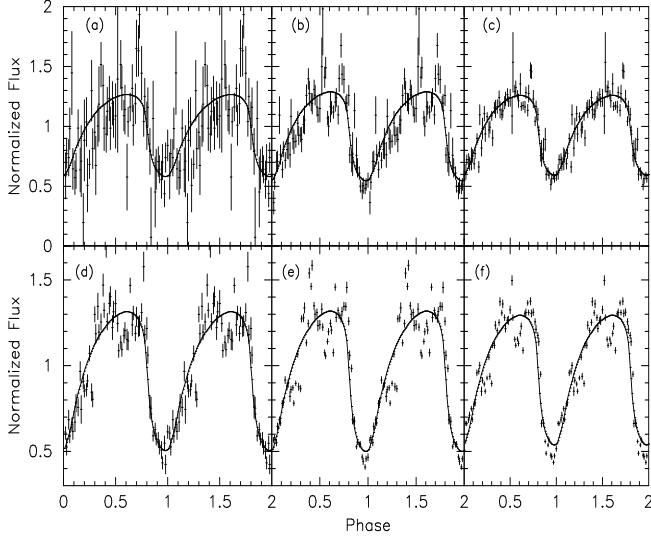


Fig. 2. The figure shows the normalized folded light curves of the source obtained from the RXTE/ASM data for different energy ranges and at different time. Upper panels (panels a, b, and c) show the folded light curves in the energy ranges 1.3–3.0 keV, 3.0–5.0 keV, and 5.0–12.1 keV for the data in the time range JD 2450086.8222 – 2450186.4878 whereas the lower panels (panels d, e, and f) show the folded light curves in the energy ranges 1.3–3.0 keV, 3.0–5.0 keV, and 5.0–12.1 keV for the data in the time range JD 2450887.2862 – JD 2450986.1345 respectively.

October 11–14 PPC observations of the source respectively. In Figure 2, we have shown the orbital modulation of the light curves along with the normalized template for two data segments of the RXTE/ASM for different energy bands. From these figures, it is observed that the shape of the orbital modulated light curves of Cygnus X-3, obtained from various observations, is similar to the shape of the normalized template.

3.2. Orbital evolution of the binary system

Figure 3 (top panel) reports the new measurements of the arrival time of the minima in the orbital modulation of the X-ray light curves of Cygnus X-3 together with those of all the previously published values (Kitamoto et al. 1987; van der Klis & Bonnet-Bidaud 1989). We have tried to fit the arrival time data with different polynomial functions. The residuals of the various polynomial fits performed on these data are also shown in other panels of the figure. The second panel of Figure 3 shows the residual of the linear fit to the arrival data whereas the third, fourth, and fifth panels of Figure 3 show the residuals of the quadratic, cubic, and sinusoidal fit to the arrival time data respectively.

The results of the various polynomial fits performed on the complete set of arrival time data are listed in Table 3. The arrival times of the orbital modulations clearly deviate from a linear relationship with the orbit num-

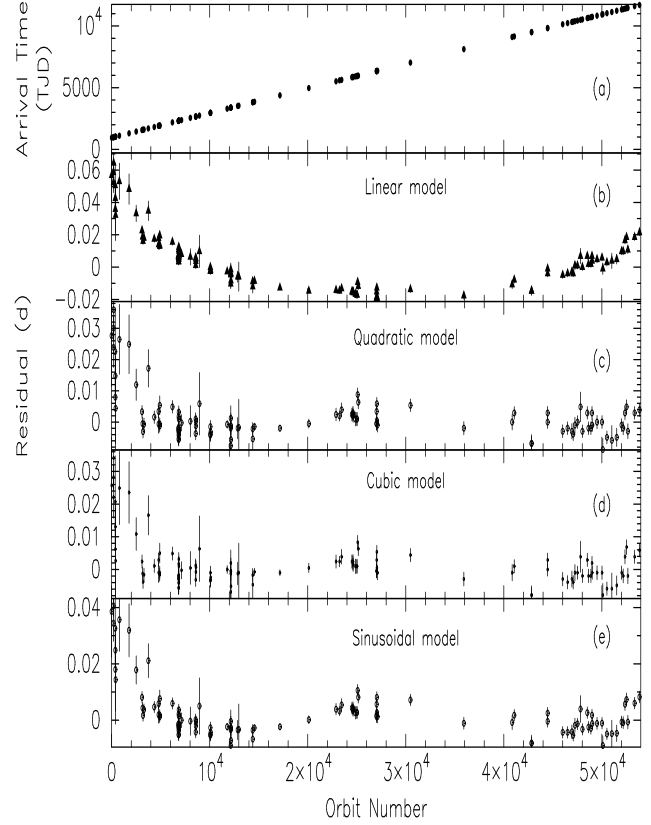


Fig. 3. The figure shows the arrival time history for the source Cygnus X-3 (top panel). The data points beyond orbit number 42830 are obtained from the present work. Arrival time residuals of the orbital modulation of the source with respect to the best-fit linear, quadratic, cubic and a linear and sinusoidal models to the data are shown in different panels.

bers. Addition of a quadratic term fits the data much better with a reduced χ^2 of 3.08 (113 dof). From the quadratic fit, the value of the period derivative is derived to be $\dot{P} = 5.76333 \times 10^{-10}$ i.e., an evolution time scale of $\dot{P}/P = 1.05419 \times 10^{-6} \text{ yr}^{-1}$. These values are similar to what was obtained with the data prior to 1993 (Kitamoto et al. 1995). A cubic model for the arrival time fits the data slightly better with reduced χ^2 of 2.96 (112 dof). However, the rate of change of \dot{P} is found to be much smaller compared to that obtained by Kitamoto et al. (1995), $\ddot{P} = -1.34008 \times 10^{-11} \text{ yr}^{-1}$. The curved feature of the residual of the linear fit to the data prompted us to fit with a model consisting of linear and sinusoidal terms as model components. Although the reduced χ^2 for this fitting is comparable to the reduced χ^2 for cubic model, the amplitude of sinusoidal component is unphysical because, according to the method described by Batten (1973), it requires the eccentricity of the binary system to be $\gg 1$. In the linear plus sinusoidal model, a reduced χ^2 of 3.5 (dof 112) was obtained by restricting the amplitude of the sinusoidal component within a physical limit so that

Table 3. The summary of the observations used to determine the ephemeris of Cygnus X-3 (New record)

Observation Period (MJD)	Satellite (detector)	Number of Orbits (p=17253 s)	Arrival time (2440000 JD+) (day)	Error in arrival time (day)
49501.91–49502.84	ASCA(GIS)	42832	9502.8736	0.0021
49501.91–49502.84	ASCA(SIS)	42832	9502.8736	0.0028
49827.99–49829.44	ROSAT(PSPC)	44466	9829.1748	0.0020
49828.59–49830.56	ROSAT(PSPC)	44470	9829.9766	0.0021
50086.32–50185.98	RXTE(ASM)	46006	10136.6934	0.0020
50186.06–50285.99	RXTE(ASM)	46506	10236.5381	0.0020
50319.46–50325.83	RXTE(PCA)	46940	10323.2031	0.0024
50348.92–50350.18	BeppoSAX(MECS1)	47074	10349.9609	0.0020
50385.00–50385.52	BeppoSAX(MECS)	47253	10385.7090	0.0025
50386.31–50485.96	RXTE(ASM)	47508	10436.6299	0.0020
50495.02–50501.12	RXTE(PCA)	47818	10498.5391	0.0047
50486.02–50585.87	RXTE(ASM)	48008	10536.4727	0.0020
50586.16–50685.95	RXTE(ASM)	48509	10636.5234	0.0020
50604.75–50717.50	RXTE(PCA)	48635	10661.6787	0.0021
50710.65–50711.26	BeppoSAX(MECS2)	48884	10711.4014	0.0020
50731.36–50731.90	BeppoSAX(MECS2)	48988	10732.1738	0.0021
50686.01–50785.73	RXTE(ASM)	49009	10736.3643	0.0020
50786.51–50883.86	RXTE(ASM)	49506	10835.6104	0.0021
50886.79–50985.63	RXTE(ASM)	50012	10936.6533	0.0020
50949.63–50954.98	RXTE(PCA)	50093	10952.8203	0.0035
50986.41–51085.89	RXTE(ASM)	50513	11036.6934	0.0020
51086.09–51185.95	RXTE(ASM)	51013	11136.5381	0.0047
51186.22–51285.96	RXTE(ASM)	51514	11236.5830	0.0029
51286.03–51385.62	RXTE(ASM)	52013	11336.2324	0.0021
51361.49–51371.77	IXAE(PPC)	52168	11367.1836	0.0021
51404.44–51404.64	RXTE(PCA)	52358	11405.1309	0.0022
51386.16–51485.96	RXTE(ASM)	52515	11436.4844	0.0023
51461.72–51464.79	IXAE(PPC)	52651	11463.6338	0.0024
51549.73–51649.73	RXTE(ASM)	53334	11600.028320	0.0020
51649.90–51749.80	RXTE(ASM)	53836	11700.274410	0.0020
51750.06–51850.02	RXTE(ASM)	54338	11800.516600	0.0020
51850.08–51948.81	RXTE(ASM)	54836	11899.958010	0.0020
51951.46–52051.45	RXTE(ASM)	55347	12002.000980	0.0020
52051.58–52151.53	RXTE(ASM)	55848	12102.048830	0.0020

$e \leq 1$. However, if a precessing eccentric orbit is the reason for the non-linear nature of the arrival times, a change in the shape of the orbital modulation of the light curve is expected, which has not been observed in the last ~ 30 years. Based on this argument, apsidal motion seems not to be an appropriate description of the arrival time data.

4. Spectral variations with orbital phases in Cygnus X-3

To investigate the spectral variations of the source during different orbital phases, we have analyzed the hardness ratios from the PPC observations with IXAE on 1999, July 3 – 13 and 1999, October 11 – 14 and the RXTE/ASM data since the beginning of the observation. From the calibration of the PPCs using Crab, it is found that the spectral data from PPC-3 is more reliable. Hence to obtain the hardness ratio (ratio of the count rate in 6 – 18 keV energy range to the count rate in 2 – 6 keV energy range), we have used the data from PPC-3. To study the spec-

tral behavior of the source at different orbital phases, we have created the time averaged profile by folding the light curves and the hardness ratio data with a period of 17253 seconds. We have plotted, in Figure 1, the orbital modulated light curves in 2 – 18 keV and 6 – 18 keV energy ranges and the hardness ratios for the 1999, July and October observations of the source.

The folded RXTE/ASM light curves in 3–5 keV and 5–12.1 keV energy bands plotted on a normalized scale with the template data and the corresponding hardness ratio for two different epochs (low and high states) are shown in Figure 3. From the PPC observations (Figure 1) and the RXTE/ASM observations (Figure 4), it is observed that, a strong binary phase dependence of the spectrum is noticed.

5. Discussion

The nature of the compact object in the binary system of Cygnus X-3 is not yet clearly understood. There are var-

Table 4. Statistics of different fitting models to the data of arrival time

Linear ephemeris: $\chi^2 = 4099$ for 114 dof	
$T_n = T_0 + Pn$	
$T_0 = 2440949.863 \pm 0.002$ JD	
$P = 0.19968775 \pm 0.00000007$ d	$\text{Cov}(T_0, P) = -2.3 \times 10^{12}$
Parabolic ephemeris: $\chi^2 = 348.3$ for 113 dof	
$T_n = T_0 + P_0n + cn^2$	$\text{Cov}(T_0, P_0) = -2.3 \times 10^{-11} d^2$
where $c = P_0\dot{P}/2$	$\text{Cov}(T_0, c) = 3.5 \times 10^{-16} d^2$
$T_0 = 2440949.892 \pm 0.001$ JD	$\text{Cov}(P_0, c) = -3.8 \times 10^{-20} d^2$
$P_0 = 0.19968443 \pm 0.00000009$ d	$\dot{P} = (5.76 \pm 0.24) \times 10^{-10}$
$c = (5.75 \pm 0.16) \times 10^{-11}$ d	$\dot{P}/P_0 = (1.05 \pm 0.04) \times 10^{-6} \text{yr}^{-1}$
Cubic ephemeris: $\chi^2 = 331$ for 112 dof	
$T_n = T_0 + P_0n + c_0n^2 + dn^3$	$\text{Cov}(T_0, P_0) = (-9.1) \times 10^{-11} d^2$
where $c_0 = P_0\dot{P}/2$ and	$\text{Cov}(T_0, c_0) = 3.1 \times 10^{-15} d^2$
$d \simeq P_0^2\dot{P}/6$	$\text{Cov}(T_0, d) = (-3.2) \times 10^{-20} d^2$
$T_0 = 2440949.8944 \pm 0.0015$ JD	$\text{Cov}(P_0, c_0) = (-5.5) \times 10^{-19} d^2$
$P_0 = 0.199684009 \pm 0.00000003$ d	$\text{Cov}(P_0, d) = 5.9 \times 10^{-24} d^2$
$c_0 = (7.7 \pm 1.1) \times 10^{-11} d$	$\text{Cov}(c_0, d) = (-2.4) \times 10^{-28} d^2$
$d = (-2.4 \pm 1.3) \times 10^{-16} d$	$\dot{P} = (7.7 \pm 1.5) \times 10^{-10}$
	$\dot{P} = (-1.3 \pm 1.6) \times 10^{-11} \text{yr}^{-1}$
Linear + Sinusoidal ephemeris: $\chi^2 = 391.1$ for 112 dof	
$T_n = T_0 + P_0n + c_0 \sin(2\pi(n - \phi)/P_{aps})$	
$T_0 = 2440949.92 \pm 0.03$ JD	
$P_0 = 0.199687 \pm 9 \times 10^{-07} d$	
$c_0 = 0.059 \pm 0.013 d$	
$\phi = 334500 \pm 6000$ no. of orbit	
$P_{aps} = 75.4 \pm 0.2$ yr	

ious arguments in the literature supporting the compact object as a massive black hole whereas some authors believe the primary companion as a neutron star. Schmutz et al. (1996) suggested that the observed time variations in the profile of infrared emission lines from the binary system are due to the orbital motion of the companion which is a Wolf-Rayet star and derived mass function for Cygnus X-3 as $2.3 M_\odot$. They obtained a range of $7-40 M_\odot$ as the mass of the compact object with a most likely value of $17 M_\odot$ and suggested that the binary system Cygnus X-3 is composed of a black hole (BH) and a Wolf-Rayet (WR) system. Several models have also been proposed to explain the lengthening of the orbital period (Bonnet-Bidaud & Chardin, 1988). Conservative mass transfer from the companion star can not explain the observations. This is due to the fact that mass accretion rate needed to produce the amount of energy emitted in X-rays and the observed orbital period change rate requires a very low mass companion $\sim 0.02 M_\odot$, which will under-fill its Roche lobe to continue mass transfer. A low mass companion star with a moderate non-conservative mass loss rate, however, can explain the period change rate, if the mass loss is due to the X-ray heating of the atmosphere. On the other hand, if the companion star is massive, the orbit may widen only if there is significant mass loss from the system in the form of strong wind and the out-flowing mass carries specific angular momentum of the primary star. The emission line rich X-ray spectrum of Cygnus X-3 detected with Chandra (Paerels et al. 2000) indicates the presence of

strongly photo-ionized stellar wind reminiscent of a high mass companion.

6. Conclusion

- We have measured 34 new minima and extended the measurement base to 30 years.
- The parabolic model provides the best fit to the new data with a modified value of \dot{P} .
- Sinusoidal model and the corresponding apsidal motion scenario is ruled out.
- Mass loss from a massive companion is most favoured in Cygnus X-3.

Acknowledgments

We thank the referees for their useful comments and suggestions that improved the contents of the paper. We acknowledge the contributions of the scientific and technical staff of TIFR, ISAC and ISTRAC for the successful fabrication, launch and operation of the IXAE. We thank Dr. S. Seetha and Dr. K. Kasturirangan for their contribution to the IXAE. It is a pleasure to acknowledge the support of Shri K. Thyagarajan, Project Director IRS-P3 satellite, Shri Tyagi, project manager of IRS-P3 and Shri J. D. Rao and his colleagues at ISTRAC. NSS thanks DST, Govt. of India, for providing the financial assistance. Work of SN is partially supported by the Kanwal Rekhi Scholarship of the TIFR Endowment Fund.

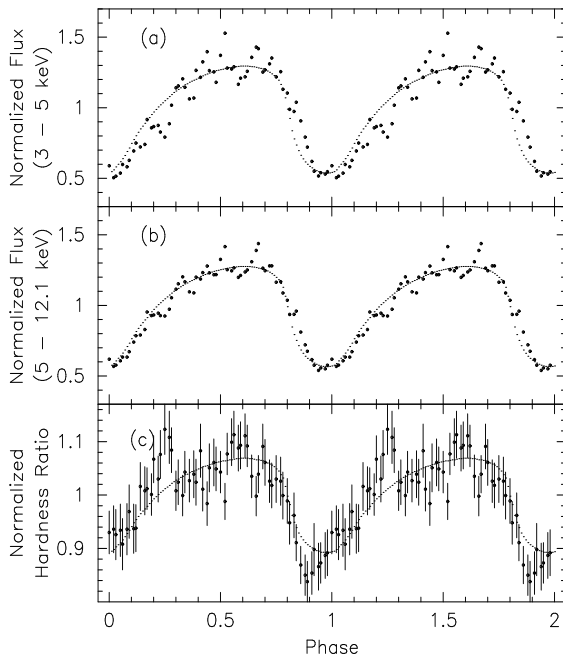


Fig. 4. The folded light curves for Cygnus X-3 with RXTE/ASM in the energy range 3–5 keV and 5–12.1 keV energy ranges along with the normalized template data are shown in panels (a) and (b). The panel (c) shows the folded hardness ratio of the source plotted on a normalized scale with the template data.

References

- Agrawal, P. C., 1998, in *Perspective in High Energy Astronomy and Astrophysics; Proceedings of the International Colloquium, Aug. 12-17, 1996 at TIFR, Mumbai*, eds: P.C. Agrawal and P.R. Viswanath, Universities Press, Hyderabad, India, p408
- Batten, A. H. 1973, in *Binary and Multiple Systems of Stars*, ed: D. Ter Harr, Pergamon Press, Oxford, New York, p86
- Bonnet-Bidaud, J. M. & Chardin, G. 1988, *PhR*, 170, 326
- Dickey, J. M. 1983, *ApJ*, 273, L71
- Elsner, R. F., Ghosh, P., Darbo, W. et al. 1980, *ApJ*, 239, 335
- Fender, R. P., Hanson, M. M., & Pooley, G. G. 1999, *MNRAS*, 308, 473
- Ghosh, P., Elsner, R. F., Weisskopf, M. C., & Sutherland, P. G. 1981, *ApJ*, 251, 230
- Hellier, C., Mason, K. O., Smale, A. P., & Kilkenney, D. 1990, *MNRAS*, 244, 39P
- Kitamoto, S., Miyamoto, S., Matsui, W., & Inoue, H. 1987, *PASJ*, 41, 81
- Kitamoto, S., Hirano, A., Kawashima, K., et al. 1995, *PASJ*, 47, 233
- Lamb, R. C., Dower, R. G., & Finkle, R. K. 1979, *ApJ*, 229, L19
- Leach, R. W., Murray, S. S., Schreier, E. J., et al. 1975, *ApJ*, 199, 184
- Mason, K. O., Becklin, E. E., Blankenship, L., et al. 1976, *ApJ*, 207, 78
- Mason, K. O., & Sanford, P. W. 1979, *MNRAS*, 189, 9P
- Parmar, A. N., Smale, A. P., Verbunt, F., & Corbet, R. H. D. 1991, *ApJ*, 366, 253
- Parmar, A. N., Oosterbroek, T., Del Sordo, S., et al. 2000, *A&A*, 356, 175
- Parsignault, D. R., Schreier, E., Grindlay, J., & Gursky, H. 1976, *ApJ*, 209, L73
- Paerels, F., Cottam, J., Sako, M., et al. 2000, *ApJ*, 533, L135
- Rao, A. R., Agrawal, P. C., Paul, B., et al. 1998, *A&A*, 330, 181
- Schmutz, W., Geballe, T. R., & Schild, H. 1996, *A&A*, 311, L25
- Singh, N. S., Singh, K. Y., Naik, S., et al. 2001, *BASI*, 29, 351
- Tavani, M., Ruderman, M., & Shaham, J. 1989, *ApJ*, 342, L31
- van den Heuvel, E. P. J., & De Loore, C. 1973, *A&A*, 25, 387
- van der Klis, M., & Bonnet-Bidaud, J. M. 1981, *A&A*, 95, L5
- van der Klis, M., & Bonnet-Bidaud, J. M. 1989, *A&A*, 214, 203
- van Kerkwijk, M. H., Charles, P. A., Geballe, T. R., et al. 1992, *Nature*, 355, 703
- White, N. E., & Holt, S. S. 1982, *ApJ*, 257, 318
- Willingale, R., King, A. R., & Pounds, K. A. 1985, *MNRAS*, 215, 295